CHEMISTRY
A European Journal

A Journal of
ChemPubSoc Europe

Accepted Article

Title: A Highly Sensitive Bimodal Detection of Amine Vapours Based on Aggregation Induced Emission of 1,2-Dihydroquinoxaline Derivatives

Authors: Parvej Alam, Nelson Lik Ching Leung, Huifang Su, Zijie Qiu, Ryan T. K. Kwok, Jacky W. Y. Lam, and Ben Zhong Tang

To be cited as: *Chem. Eur. J.* 10.1002/chem.201703253

Link to VoR: http://dx.doi.org/10.1002/chem.201703253

Supported by
ACES

WILEY-VCH

10.1002/chem.201703253

WILEY-VCH

FULL PAPER

A Highly Sensitive Bimodal Detection of Amine Vapours Based on Aggregation Induced Emission of 1,2-Dihydroquinoxaline Derivatives

Parvej Alam[+],[a, b] Nelson L. C. Leung[+],[a, b] Huifang Su,[a, b] Zijie Qiu,[a, b] Ryan T. K. Kwok,[a, b] Jacky W. Y. Lam,[a, b] and Ben Zhong Tang*[a, b, c]

Abstract: The detection of food spoilage is a major concern in food safety as large amounts of food are transported globally. Direct analysis of food samples is often time-consuming and requires expensive analytical instrumentation. A much simpler and more cost-effective method for monitoring food fermentation is to detect biogenic amines generated as a by-product during food decomposition. In this work, a series of 1,2-dihydroquinoxaline derivatives (DQs) with aggregation-induced emission (AIE) characteristics were synthesized and their protonated forms, i.e. H^+DQs, can be utilized for the sensitive detection of biogenic amines. For example, upon exposure to amine vapours, deprotonation occurs which converts the red-coloured, non-emissive H^+DQ2 back to its yellow-coloured, fluorescent parent form. The bimodal absorption and emission changes endow the system with high sensitivity, capable of detecting ammonia vapour at a concentration of as low as 690 ppb. Taking advantage of this, H^+DQ2 was successfully applied for the detection of food spoilage and was established as a robust and cost effective technique to monitor food safety.

[a] Dr. P. Alam,[+] N. L. C. Leung,[+] Dr. Huifang Su, Z. Qiu, Dr. R. T. K. Kwok, Dr. J. W. Y. Lam, Prof B. Z. Tang
HKUST Shenzhen Research Institute
No. 9 Yuexing 1st Rd, South Area, Hi-tech Park,
Nanshan, Shenzhen 518057, China
E-mail: tangbenz@ust.hk

[b] Dr. P. Alam,[+] N. L. C. Leung,[+] Dr. Huifang Su, Z. Qiu, Dr. R. T. K. Kwok, Dr. J. W. Y. Lam, Prof B. Z. Tang
Department of Chemistry
Division of Biomedical Engineering
Hong Kong Branch of Chinese National Engineering Research Center for Tissue Restoration and Reconstruction
Institute for Advanced Study
Institute of Molecular Functional Materials and State Key Laboratory of Molecular Neuroscience
The Hong Kong University of Science and Technology
Clear Water Bay, Kowloon, Hong Kong, China

[c] Prof B. Z. Tang
Guangdong Innovative Research Team
SCUT-HKUST Joint Research Laboratory
State Key Laboratory of Luminescent Materials and Devices
South China University of Technology
Guangzhou 510640, China

[+] P.A. and N.L.C.L. contributed equally to this work.

Supporting information, including NMR spectra, mass spectra, absorption and emission spectra, AIE PL curves, absorption and emission spectra changes after protonation of DQ2, Job plot of DQ2, PL reversibility of H^+DQ2, calculated average intensity plot after exposure to ammonia vapour, photograph of H^+DQ2 filter paper strip sealed with salmon sample at room temperature and 2 °C, and photographs H^+DQ2 filter paper strip sealed with white-leg shrimp for this article can be found under <DOI>

Introduction

Over USD $220 billion worth of meat and seafood was shipped all over the world in 2016.[1] Because of this, food safety and human health are fundamentally important issues. Much research has been done to ensure that the transported food remains fresh and unspoiled,[2] and many methods have been designed to monitor the safety of food products.[3] For example, time-temperature indicators (TTI)[4] have been developed to show whether raw food materials have been exposed to elevated temperatures for an extended duration of time. Indeed, even the FDA has adopted guidelines for the use of TTIs in US seafood products to ensure food safety.[5] However, maintaining a chilled temperature only slows down the enzymatic processes of food spoilage. In fact, biogenic amine species, such as putrescine and cadaverine, produced by microbes have been found in rainbow trout stored at 0 °C by the second day.[6] Biogenic amines have gained recognition as good indicators of food freshness because they are products of microbial fermentation.[7] In the process of food spoilage, microbes break down amino acids *via* deaminization to generate ammonia and decarboxylation to generate biogenic amines such as cadaverine, putrescine, spermidine, spermine, and others (Scheme 1). Biogenic amines not only signal the freshness of the food, but also have adverse impact on human health and physiological functions.[8] In fact, putrescine, cadaverine, spermidine, and spermine can react with nitrites to generate nitrosamines, a known carcinogen, in processes such as meat curing.[9]

Thus, monitoring biogenic amines in food is important because the chemical species and their by-products can have toxic effects and they also signify food spoilage by microbes. Compared to TTIs, a system that can detect the presence of biogenic amines is a more direct method to monitor food safety and hygiene. One obstacle for the detection of biogenic amines is that they have no inherent characteristic absorption or emission. There are many conventional techniques for amine detection[10] such as GC-MS,[11] electrochemical systems,[12] array systems,[13] and HPLC,[14] but many of these are more complex in nature.

The detection of biogenic amines can be simplified by exploiting the chemical nature of the amines to induce photophysical changes. For example, colourimetric change can be induced by protonation/deprotonation[15] or through chemical reaction with the probe.[16] Such a change allows easy visualization of the presence of biogenic amines. A further improvement would be if the system shows luminescence change upon exposure to amine vapours as well.[17]

10.1002/chem.201703253

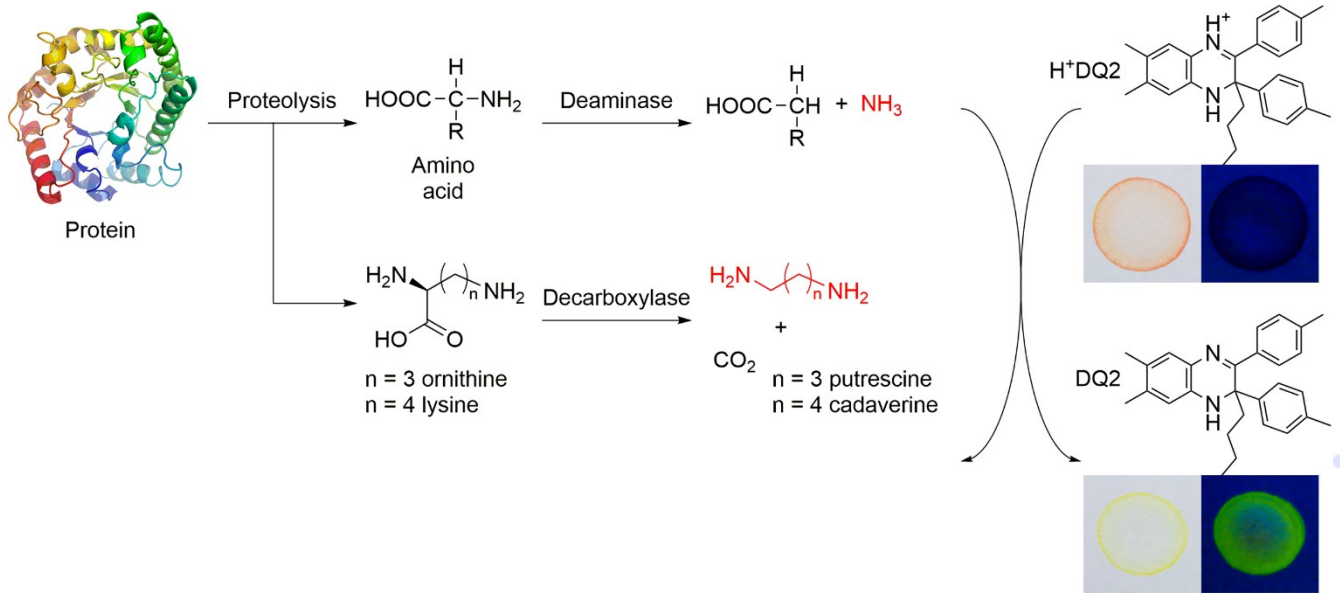

Scheme 1. Schematic illustration of microbial proteolysis leading to the generation of ammonia and selected biogenic amines. Ammonia and biogenic amines deprotonate red-coloured, non-emissive H^+DQ2 to form yellow-coloured, fluorescent DQ2, allowing the detection of food spoilage. Structures of H^+DQ2 and DQ2 and their photos taken under (left) daylight and (right) 365 nm UV irradiation.

Luminescent systems exhibit high sensitivity in response to external stimuli. For example, amine detection showing absorption and luminescence changes in solution with nanomolar sensitivity has recently been reported.[18] Solution-based systems are hard to use due to inherent logistic issues. Ideally, loading the chemical sensor onto a solid support would drastically simplify the methodology.[19] This allows the sensor to be sealed within the packaging for a more direct monitoring of food freshness. Unfortunately, conventional luminescent systems often experience reduced emission intensity in the aggregate state due to aggregation-caused quenching (ACQ).[20] In contrast, dye molecules with aggregation-induced emission (AIE)[21] characteristics are not affected by the ACQ effect and show strong light emission in the solid state, making them ideal candidates as sensors for detecting biogenic amines.[22] The bulky nature of AIEgens may even enhance the sensitivity due to the increase in intermolecular void spaces facilitating analyte species to reach the chemical sensors.

Herein, we report the synthesis of a series dihydroquinoxaline derivatives (DQ1-4) with both AIE and intramolecular charge transfer (ICT) features displaying strong solid-state emission. Among the DQ derivatives, DQ2 was selected as a model for the investigation due to its abundance (Scheme 1). DQ2 is yellow in colour and after protonation to form H^+DQ2, its colour visibly changes to red. In addition, H^+DQ2 is non-emissive but emission is recovered after deprotonation. This provides both a colourimetric change and emission turn-on feature for sensitive amine sensing with a detection limit of 690 ppb for ammonia (NH_3). In particular, H^+DQ2 was responsive even to biogenic amines such as putrescine, cadaverine and spermidine. Because of its AIE nature, the probe can be loaded onto a solid substrate and sealed in a container with food. As the food ferments, biogenic amines released induces both colourimetric change and emission turn-on of DQ2, allowing easy visualization for food safety monitoring.

Results and Discussion

Characterization and Photophysical Properties

The DQs were synthesized by condensations of 1,2-diamino-4,5-disubstituted benzenes (**1**) and benzil derivatives (**2**) followed by reaction of the resulting intermediates (**3**) with *n*-butyl lithium (*n*-BuLi) (Scheme 2). All the compounds were obtained in good to moderate yields. Their chemical structures were confirmed by standard spectroscopic techniques including NMR and HRMS (Figure S1-S4 in the Electronic Supporting Information) with satisfactory results. The reaction of **3** with *n*-BuLi converts an imine (sp^2 nitrogen, electron accepter) to an amine (sp^3 nitrogen, electron donor). This creates a donor (D)-acceptor (A) structure in the DQs.

The optical properties of the DQ derivatives were studied in organic solvents with different polarities at room temperature (Figure S5-8). The DQs show an absorbance band in the range of 380-420 nm. Their emission spectra changed with the solvent because of the ICT effect stemming from their D-A structures. The ICT features of the compounds were further investigated by DFT-based calculations using Jaguar 9.4 in Schrödinger Materials Science Suite 2016-4.[23] Results showed that the HOMO cloud was localized mainly at the dihydropyrazine *amine* and the fused phenyl ring while the LUMO cloud was spread over the dihydropyrazine *imine* and other phenyl rings (Figure S9). As such, ICT is likely to arise from this D-A structure. The calculated energy gaps were in the range of 3.50-3.70 eV.

10.1002/chem.201703253

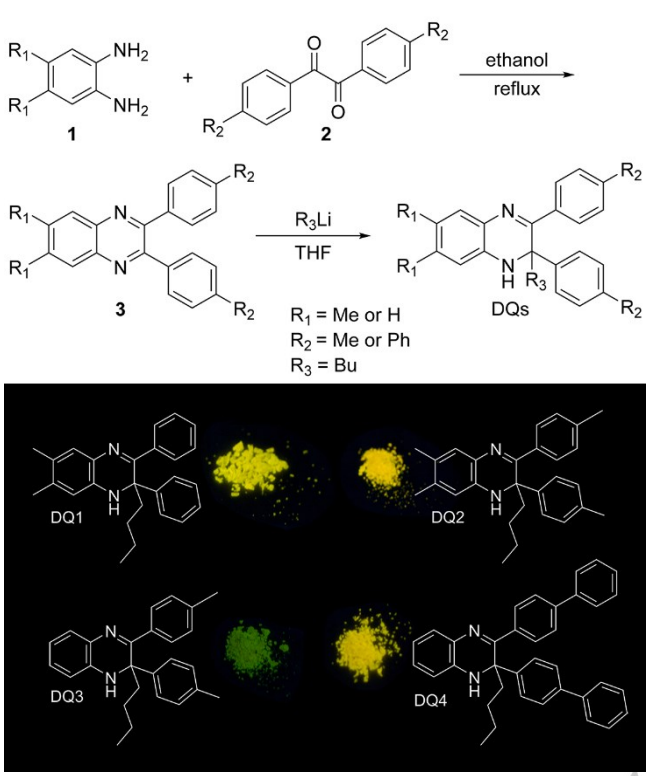

Scheme 2. Top: Synthetic route for the dihydroquinoxaline (DQ) derivatives. Bottom: Fluorescent photo of the DQs taken under 365 nm UV excitation.

The AIE properties of the DQs were further studied in methanol/water (Figure 1, S10, S13 and S15) and THF/water mixtures (Figure S11, S12, S14 and S16). With an increase in water fraction from 0 to 60% in methanol/water mixture, the emission decreased alongside a bathochromic shift in peak maximum from 573 nm to 585 nm (Figure 1). This phenomenon is attributed to the enhancement of the ICT effect by the increase in solvent polarity. However, at f_w = 70%, an immediate 28-fold emission enhancement was observed with a hypsochromic shift in the PL spectrum. Further addition of water strengthens the blue-shifted emission. The PL enhancement at $f_w \geq 70\%$ was recognized as a signal for the activation of the AIE phenomenon due to the formation of aggregates.[21] Similar observations were found upon the addition of water to the THF solution of DQ2 (Figure S12). These results clearly demonstrate that DQ2 exhibits both typical AIE and ICT features. The emission enhancement after aggregate formation was due to the predominance of the AIE effect over the ICT effect. Analogous AIE behaviour was observed for other DQs (Figure S10-16).

Protonation-Induced Photophysical Changes

Due to the D-A structure of the DQs, we anticipated that their optical properties would change when their imine unit is protonated. On the other hand, deprotonation of the aforementioned nitrogen by amine vapours may restore the original properties of the molecules.

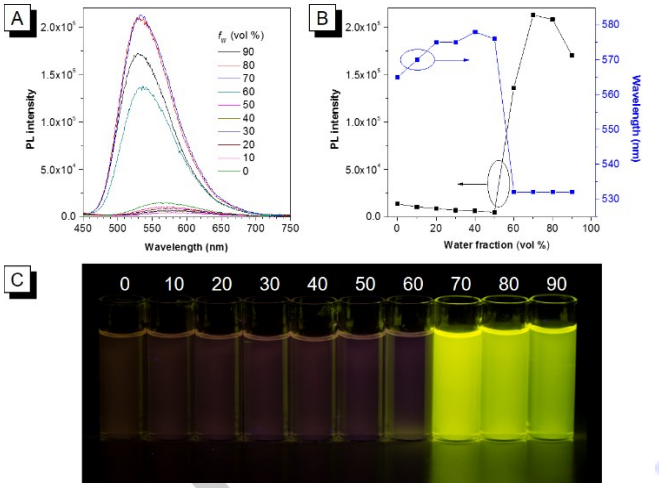

Figure 1. (A) PL spectra of DQ2 in MeOH/H_2O mixtures with different water fractions (f_w). Concentration: 10 μM; λ_{ex} = 400 nm. (B) Plot of PL intensity and emission maximum versus the composition of the MeOH/H_2O mixtures of DQ2. (C) Fluorescent image of DQ2 in MeOH/H_2O mixtures with water fractions from 0 to 90% (left to right) taken under 365 nm UV irradiation.

To verify these hypotheses, DQ2 was first reacted with trifluoroacetic acid (TFA) to generate H^+DQ2, the protonated form of DQ2 (Scheme 1). The optical properties of both DQ2 and H^+DQ2 were then investigated. The absorption spectrum of DQ2 in DCM showed two peaks at 270 nm and 392 nm, which moved to 338 nm and 478 nm, upon the addition of TFA (Figure S17). PL analysis showed a similar result where the emission maximum moved from 530 nm to 560 nm upon molecular protonation (Figure S18). The ICT effect of the molecular was strengthened upon protonation, which might account for the red-shift in the absorption and emission. It should be noted that alongside the wavelength shift, the emission intensity is also significantly quenched. In addition, the absorption spectrum of H^+DQ2 significantly overlap with its PL spectrum. Thus, the non-emissive nature of H^+DQ2 may be explained as a combination of self-absorption and the photoinduced electron transfer effect (Figure S18). The addition of base such as triethylamine (TEA) restores of the emission peak at 530 nm.

The stoichiometric ratio between DQ2 and TFA was determined to be 1:1 by UV-VIS titration followed by a Job plot (Figure S19). The protonation process was also monitored using NMR spectroscopy: after the addition of TFA the resonance peak at δ 6.18 ppm shifted to 6.50 ppm, which moved to the original position after deprotonation with TEA (Figure S17). These experiments showed the protonation and deprotonation processes are reversible in nature.

We prepared H^+DQ2-loaded filter paper to investigate the system's ability to detect amine vapours in the solid state. Whatman glass microfibre filters were chosen as a substrate for their porosity and we were careful to only deposit 100 μL of a 100 μM DCM solution to ensure accuracy and reproducibility. Its reversibility was tested by exposing alternatively to NH_3 and TFA for multiple cycles (Figure S20). No emission was initially observed from the filter paper but a turn-on signal appears after

10.1002/chem.201703253

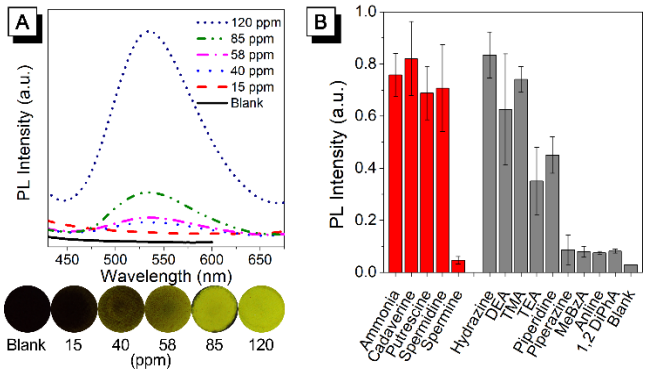

Figure 2. (A) Top: PL spectra of H⁺DQ2-doped filter paper strips after exposure to 0 ppm, 15 ppm, 40 ppm, 58 ppm, 85 ppm, and 120 ppm of ammonia vapour for 5 min. λ_{ex} = 365 nm. Below: Photographs of the H⁺DQ2-doped filter paper strips after exposure to ammonia vapour taken under 365 nm UV excitation. (B) PL turn-on response of H⁺DQ2-loaded filter paper strip in the presence of various amine vapours. H⁺DQ2 was exposed to aqueous or methanolic amine solutions (0.08 M) for 40 s. Biogenic amines and ammonia coloured in red, other amine species coloured grey. Ammonia was prepared as an aqueous solution, while other amine species were prepared as methanolic solutions. Abbreviation: DEA = diethylamine; TMA = trimethylamine; TEA = triethylamine; MeBzA = methylbenzylamine; 1,2 DiPhA = 1,2-diphenylamine.

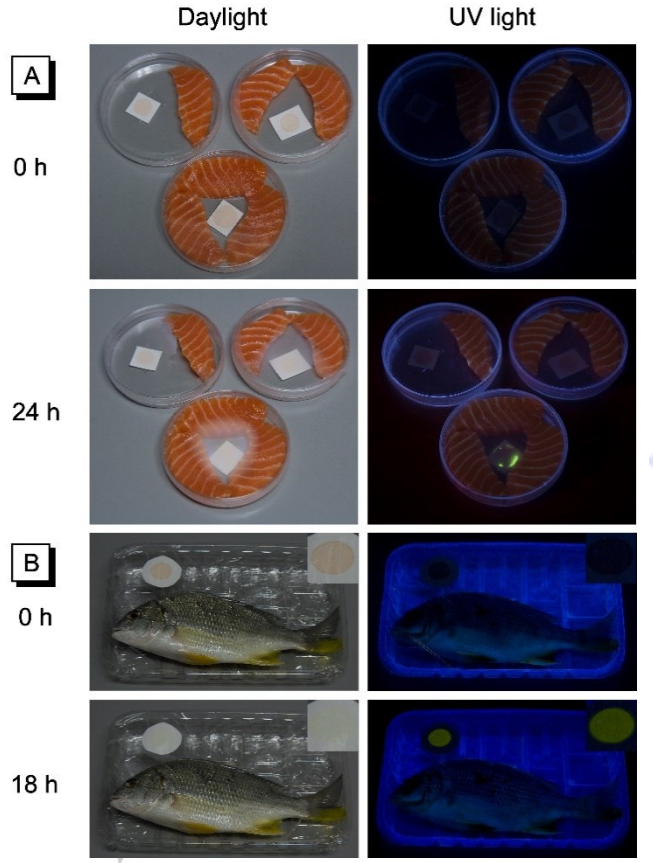

Figure 3. (A) H⁺DQ2 sensor sealed with salmon sashimi in room temperature. After 24 hours, emission turn-on can be observed. (B) H⁺DQ2 sensor in sealed packages of yellowfin seabream, after 18 hours, emission turn-on can be observed. Inset: magnified photo of the sealed sensor.

fuming with ammonia gas. The emission faded again after exposure to TFA vapour. Such emission turn-on and turn-off can be repeated for many cycles with minimal fatigue, demonstrating the high reversibility and reliability of the present system.

To investigate the turn-on sensitivity, the H⁺DQ2-loaded strips were exposed to various concentrations of NH_3 vapour. 5 mL of aqueous NH_3 solutions with various concentrations were placed in 100 mL bottles and sealed overnight to reach equilibrium. The NH_3 vapour concentrations were measured using Gastec detector tubes and the vapours were exposed to the H⁺DQ2-loaded strips. The turn-on emissions were measured using PL spectroscopy (Figure 2A). The strips can show varying PL intensities due to inherent microscopic differences of the substrate. As such, instead of using a spectrophotometer to measure a single location, the average greyscale values of the strips were also calculated using MATLAB to represent the overall brightness of the fluorescent images.[24] These values were then used to determine the limit of detection (LOD). First, a regression line was obtained by plotting the greyscale value versus the amine concentration. The LOD was calculated to be 690 ppb by the equation $3\sigma/m$, where σ is the standard deviation of the blank measurement and m is the slope of the regression line. (Figure S21).

Fluorescence Detection of Inorganic and Biogenic Amines

The fluorescence turn-on capability of the H⁺DQ2-loaded filter paper strip was further investigated using different amine vapours. 10 mL of 0.08 M methanolic solutions of hydrazine, diethylamine (DEA), trimethylamine (TMA), triethylamine (TEA), piperidine, piperazine, methylbenzylamine (MeBzA), aniline, 1,2-diphenylamine (1,2 DiPhA), cadaverine, putrescine, spermidine, and spermine were prepared in 25 mL glass vials. A 10 mL of 0.08M aqueous solution of ammonia was also prepared. The H⁺DQ2-loaded filter papers were then placed on top of the open glass vials of the amine solutions for 40 s. After exposure, the fluorescence of the filter papers was measured. The filter paper was then exposed to TFA vapour to re-protonate DQ2. This finishes one detection cycle. A total of three detection cycles were performed for each amine solution and the PL responses were graphed in Figure 2B. The filter paper strips showed a turn-on response within 40 seconds after exposure to ammonia, cadaverine, putrescine, spermidine along with hydrazine, TEA, DEA, TMA and piperidine. Less volatile amine species such as spermine, piperazine, MeBzA, aniline, and 1,2 DiPhA, induced smaller emission changes.

These experiments revealed the potentiality of H⁺DQ2-loaded filter paper as a turn-on fluorescence sensor for volatile amines including important biogenic amines.

Detection of Amines from Food Spoilage

Based on the capability of H⁺DQ2-loaded filter paper for detecting biogenic amines, we aimed to test the system's response to vapour biogenic amines generated in-situ due to fermentation. Fresh samples of salmon sashimi, yellowfin seabream, and white-leg shrimp were purchased from a local supermarket. To first examine if the test strip would show any response, three sealed

Petri dishes with test strips containing (i) no sample and samples of salmon sashimi kept at (ii) room temperature and (iii) 2 °C were prepared (Figure S22). After 48 h, only the test strip sealed with the sashimi kept at room temperature showed colour and emission change. Its original red colour changed to yellow and bright emission was observed under UV irradiation. Further testing of the strips was performed by sealing the strips with varying numbers of fresh salmon sashimi at room temperature (Figure 3A). After 24 h, the test strip sealed with three pieces of salmon sashimi was somewhat emissive, although *no* apparent colour change was observed. After 48 h, all test strips showed both visible colour change and emission turn-on. This highlights the higher sensitivity of fluorescence technique over colourimetric change for detecting biogenic amines. Fluorescence turn-on can be observed before visible colourimetric change. The threshold for fluorescence turn-on can be reached faster in the sample with a larger sample size, leading to visible emission after 24 h. Apparent colour change indicates that active fermentation has taken place.

To further explore the capability and ease of use of the test strips, we attached them to plastic wrap used to reseal the package of yellowfin seabream (Figure 3B) and white-leg shrimp (Figure S23). After keeping the samples at room temperature for 18 h, absorption and fluorescence changes were observed in both samples, which were indicative of microbial fermentation. The strips are easy to produce providing simple and sensitive monitoring of food fermentation.

Conclusions

In this work, we developed a series of DQs with both AIE and ICT features. DQs show absorption and emission changes upon protonation. Utilizing this bimodal variation, DQs were used as sensors for sensitive detection of biogenic amine vapours such as cadaverine, putrescine and spermidine. The detection limit was found to be 690 ppb for NH_3, which was low enough to detect amines generated from food spoilage. An easily prepared portable sensor was developed by using filter paper as a solid support to detect food spoilage. The sensor displays changes in its optical properties in response to amines produced due to food spoilage: luminescent turn-on can give the earliest signal for the presence of fermentation, and colourimetric changes allow easy visualization with just the naked eye. It is noteworthy that DQ2 can easily enter HeLa cells and stain lipid droplets with high brightness and specificity (Figure S24). MTT assay showed that even at concentration of up to 10 μM, DQ2 showed minimal cytotoxicity to cells (Figure S25). Its low cytotoxicity is particularly important as a food safety monitoring agent. Thus, new materials synthesized in this study are expected to find an array of advanced applications.

Experimental Section

Materials

4,5-Dimethylbenzene-1,2-diamine, benzene-1,2-diamine, 1,2-di-p-tolylethane-1,2-dione, 1,2-bis(4-bromophenyl)ethane-1,2-dione and ethanol were purchased from the J&K Company Ltd. All spectroscopic grade solvents: such as dichloromethane (DCM), methanol (MeOH), toluene, 1,4-dioxane, ethyl acetate, chloroform ($CHCl_3$), tetrahydrofuran (THF), acetonitrile (ACN), dimethylformamide were procured from the Merck Company. Whatman glass microfibre filter paper was used for the H^+DQ2-loaded filter paper strips.

General Syntheses of 2,3-diphenylquinoxaline derivatives (3)

Intermediate **3** was synthesized based on reported works[25] with the synthetic route shown in Scheme 2. To a stirred solution of 1,2-diamino-4,5-disubstituted benzenes (**1**, 18.5 mmol) in ethanol (50 mL), benzil derivatives (**2**, 18.5 mmol) and a catalytic amount of acetic acid were added. The mixture was refluxed for 5 h. After cooling to room temperature and solvent evaporation, the crude product was purified by recrystallization from a mixture of DCM and ethanol (1:5), generating **3** in 70-80% yield.

General Syntheses of 1,2-dihydroquinoxaline (DQ) derivatives

An oven dried round bottom flask sealed with rubber stopper was charged **3** (1.6 mmol) followed by addition of dry THF (30 mL). The reaction mixture was cooled at 0 °C, and *n*-butyl lithium (1.2 mmol, 2.5 M in hexane) was added dropwise to the mixture using a syringe. After complete addition, the reaction mixture was stirred at room temperature for 3 h. Then, the mixture was hydrolysed by addition of an excess amount of water. The reaction mixture was extracted using CH_2Cl_2 and dried over sodium sulphate. The solvent was evaporated under reduced pressure to afford the crude product which was further purified by column chromatography using ethyl acetate/hexane mixture as eluent to give a solid product in 55-70% yield.

Characterization

^1H and ^{13}C spectra were recorded on a Bruker ARX 400 NMR spectrometer using $CDCl_3$ and MeOD solvents. UV-VIS absorption spectra were recorded on a PerkinElmer UV/VIS Lambda 365. The photoluminescence (PL) spectra were recorded on a Fluorolog®-3 spectrofluorometer. High-resolution mass spectroscopy (HRMS) were carried out on a GCT premier CAB048 mass spectrophotometer operating in MALDI-TOF mode. All the reactions were performed under nitrogen atmosphere and the progress of the reaction was monitored using thin-layer chromatography (TLC) plates pre-coated with 0.20 mm silica gel.

DQ1: ^1H NMR (400 MHz, $CDCl_3$) δ (ppm) 7.56-7.50 (m, 2H), 7.39-7.26 (m, 6H), 7.21 (ddd, *J* = 8.2, 6.3, 2.2 Hz, 3H), 6.24 (s, 1H), 3.75 (s, 1H), 2.40-2.26 (m, 1H), 2.18 (d, *J* = 10.1 Hz, 6H), 2.03-1.81 (m, 1H), 1.71 (m, 1H), 1.36-1.09 (m, 3H), 0.77 (t, *J* = 7.1 Hz, 3H); ^{13}C NMR (101 MHz, $CDCl_3$) δ (ppm) 161.60, 145.40, 138.78, 137.73, 133.61, 129.39, 129.23, 128.92, 128.82, 128.17, 127.75, 127.73, 126.15, 125.73, 113.74, 61.59, 37.75, 26.65, 22.98, 19.84, 18.83, 13.85. MS (MALDI-TOF): calcd. for M^+ = *m*/*z* 368.2252; found: *m*/*z* 368.2255.

DQ2: ^1H NMR (400 MHz, $CDCl_3$) δ (ppm) 7.39 (d, *J* = 8.2 Hz, 2H), 7.23 (d, *J* = 8.2 Hz, 2H), 7.14 (d, *J* = 8.8 Hz, 3H), 7.00 (d, *J* = 8.0 Hz, 2H), 6.19 (s, 1H), 3.66 (s, 1H), 2.31 (d, *J* = 14.1 Hz, 6H), 2.15 (d, *J* = 11.4 Hz, 6H), 2.01-1.81 (m, 1H), 1.76-1.53 (m, 1H), 1.34-1.04 (m, 3H), 0.75 (t, *J* = 7.0 Hz, 3H); ^{13}C NMR (101 MHz, $CDCl_3$) δ (ppm) 160.98, 142.19, 138.10, 136.79, 136.72, 135.41, 133.00, 128.93, 128.79, 128.47, 127.76, 127.50, 125.35, 124.89, 112.98, 60.63, 37.47, 26.06, 22.40, 20.64, 20.43, 19.16, 18.16, 13.25. MS (MALDI-TOF): calcd. for $(M+H)^+$ = *m*/*z* 397.2644; found: *m*/*z* 397.2614.

DQ3: ^{1}H NMR (400 MHz, MeOD) δ (ppm) 7.35 (d, *J* = 8.3 Hz, 2H), 7.18 (dd, *J* = 11.2, 4.8 Hz, 3H), 7.11 (d, *J* = 8.1 Hz, 2H), 7.04 (d, *J* = 8.1 Hz, 2H), 6.91 (td, *J* = 7.8, 1.4 Hz, 1H), 6.54 (td, *J* = 7.6, 1.2 Hz, 1H), 6.47 (dd, *J* = 7.9, 1.1 Hz, 1H), 3.30 (s, 1H), 2.28 (d, *J* = 3.5 Hz, 6H), 2.20 (m, 1H), 2.04 (m,1H), 1.77-1.58 (m, 1H), 1.31-1.02 (m, 2H), 0.72 (t, *J* = 7.1 Hz, 1H); ^{13}C NMR (101 MHz, $CDCl_3$) δ (ppm) 162.01, 142.01, 138.37, 136.90, 135.35, 135.19, 130.59, 128.97, 128.22, 127.82, 127.62, 127.57, 125.42, 117.07, 111.72, 60.68, 37.50, 26.06, 22.39, 20.66, 20.43, 13.26. MS (MALDI-TOF): calcd. for $(M+H)^+$ = *m*/*z* 369.2331; found: *m*/*z* 369.2321.

DQ4: ^{1}H NMR (400 MHz, $CDCl_3$) δ (ppm) 7.64-7.53 (m, 8H), 7.46 (d, *J* = 4.4 Hz, 4H), 7.45-7.38 (m, 5H), 7.34 (q, *J* = 7.2 Hz, 2H), 7.02 (td, *J* = 7.7, 1.4 Hz, 1H), 6.73 (td, *J* = 7.6, 1.2 Hz, 1H), 6.43 (dd, *J* = 7.9, 1.1 Hz, 1H), 3.91 (s, 1H), 2.54-2.38 (m, 1H), 2.11-1.95 (m, 1H), 1.85-1.69 (m, 1H), 1.27 (m, 3H), 0.78 (t, *J* = 7.1 Hz, 3H); ^{13}C NMR (101 MHz, $CDCl_3$) δ (ppm) 161.96, 144.29, 141.68, 140.58, 140.42, 140.25, 137.40, 135.87, 131.22, 130.36, 129.16, 128.84, 128.78, 128.73, 128.47, 127.62, 127.53, 127.02, 127.01, 126.61, 126.49, 117.95, 112.50, 61.44, 38.11, 26.75, 23.02, 13.89. MS (MALDI-TOF): calcd. for $(M+H)^+$ = *m*/*z* 493.2644; found: *m*/*z* 493.2632.

Computational Methods

The DFT calculations were performed using Jaguar 9.4 in Schrödinger Materials Science Suite 2016-4.[23] B3LYP functional was used to optimize the structures of DQ1-4 using the 6-31G** basis set.

Acknowledgements

This work was partially supported by the National Basic Research Program of China (973 Program, 2013CB834701 and 2013CB834702), the University Grants Committee of Hong Kong (AoE/P-03/08), the Research Grants Council of Hong Kong (16305015, 16308016, and N_HKUST604/14), the Innovation and Technology Commission (ITC-CNERC14SC01 and ITCPD/17-9). We thank the support of the Guangdong Innovative Research Team Program (201101C0105067115) and the Science and Technology Plan of Shenzhen (JCYJ20160229205601 4di82).

Keywords: aggregation-induced emission • amines • colourimetric • fluorescence • food safety

[1] a) I. T. Centre, Trade Map - List of importers for the selected product in 2016 (Fish and crustaceans, molluscs and other aquatic invertebrates), http://www.trademap.org/tradestat/Country_SelProduct.aspx?nvpm=1|||||03|||2|1|1|1|1||2|1|, accessed: May 2017; b) I. T. Centre, Trade Map - List of importers for the selected product in 2016 (Meat and edible meat offal), http://www.trademap.org/tradestat/Country_SelProduct.aspx?nvpm=1|||||02|||2|1|1|1|1||2|1|, accessed: May 2017.

[2] a) M. Friedman, *J. Agric. Food Chem.* **1996**, *44*, 631-653; b) L. Gram, L. Ravn, M. Rasch, J. B. Bruhn, A. B. Christensen, M. Givskov, *Int. J. Food Microbiol.* **2002**, *78*, 79-97.

[3] a) Y. Wang, T. V. Duncan, *Curr. Opin. Biotechnol.* **2017**, *44*, 74-86; b) M. Akhoundian, A. Rüter, S. Shinde, *Sensors* **2017**, *17*, 645.

[4] a) M. Ozdemir, J. D. Floros, *Crit. Rev. Food Sci. Nutr.* **2004**, *44*, 185-193; b) A. Mills, D. Hawthorne, A. Graham, K. Lawrie, *Chem. Commun.* **2016**, *52*, 13987-13990; c) P. S. Taoukis, T. P. Labuza, *J. Food Sci.* **1989**, *54*, 783-788.

[5] FDA, Fish and Fishery Products Hazards and Controls Guidance, https://www.fda.gov/downloads/Food/GuidanceRegulation/UCM251970.pdf, accessed: May 2017.

[6] A. A. Dawood, J. Karkalas, R. N. Roy, C. S. Williams, *Food Chem.* **1988**, *27*, 33-45.

[7] a) C. Ruiz-Capillas, F. Jiménez-Colmenero, *Crit. Rev. Food Sci. Nutr.* **2005**, *44*, 489-599; b) I. A. Bulushi, S. Poole, H. C. Deeth, G. A. Dykes, *Crit. Rev. Food Sci. Nutr.* **2009**, *49*, 369-377; c) M. T. Veciana-Nogués, A. Mariné-Font, M. C. Vidal-Carou, *J. Agric. Food Chem.* **1997**, *45*, 2036-2041; d) F. a. A. O. o. t. U. Nations, W. H. Organization, *Joint FAO/WHO expert meeting on the public health risks of histamine and other biogenic amines from fish and fishery products: meeting report*, World Health Organization, Geneva, **2013**.

[8] A. R. Shalaby, *Food Res. Int.* **1996**, *29*, 675-690.

[9] a) J. J. Warthesen, R. A. Scanlan, D. D. Bills, L. M. Libbey, *J. Agric. Food Chem.* **1975**, *23*, 898-902; b) G. Drabik-Markiewicz, B. Dejaegher, E. De Mey, T. Kowalska, H. Paelinck, Y. Vander Heyden, *Food Chem.* **2011**, *126*, 1539-1545.

[10] A. Önal, *Food Chem.* **2007**, *103*, 1475-1486.

[11] a) J. O. Fernandes, I. C. Judas, M. B. Oliveira, I. M. P. L. V. O. Ferreira, M. A. Ferreira, *Chromatographia* **2001**, *53*, S327-S331; b) S. C. Cunha, M. A. Faria, J. O. Fernandes, *J. Agric. Food Chem.* **2011**, *59*, 8742-8753.

[12] L. K. Fiddes, J. Chang, N. Yan, *Sensor Actuat. B-Chem.* **2014**, *202*, 1298-1304.

[13] a) G. A. Sotzing, J. N. Phend, R. H. Grubbs, N. S. Lewis, *Chem. Mater.* **2000**, *12*, 593-595; b) J. Lange, C. Wittmann, *Anal. Bioanal. Chem.* **2002**, *372*, 276-283.

[14] a) N. Innocente, M. Biasutti, M. Padovese, S. Moret, *Food Chem.* **2007**, *101*, 1285-1289; b) S. Gómez-Alonso, I. Hermosín-Gutiérrez, E. García-Romero, *J. Agric. Food Chem.* **2007**, *55*, 608-613.

[15] N. A. Rakow, A. Sen, M. C. Janzen, J. B. Ponder, K. S. Suslick, *Angew. Chem. Int. Ed.* **2005**, *44*, 4528-4532.

[16] V. Valderrey, A. Bonasera, S. Fredrich, S. Hecht, *Angew. Chem. Int. Ed.* **2017**, *56*, 1914-1918.

[17] A. Mallick, B. Garai, M. A. Addicoat, P. S. Petkov, T. Heine, R. Banerjee, *Chem. Sci.* **2015**, *6*, 1420-1425.

[18] S. Mallick, F. Chandra, A. L. Koner, *Analyst* **2016**, *141*, 827-831.

[19] A. Sandeep, V. K. Praveen, K. K. Kartha, V. Karunakaran, A. Ajayaghosh, *Chem. Sci.* **2016**, *7*, 4460-4467.

[20] X. Ma, R. Sun, J. Cheng, J. Liu, F. Gou, H. Xiang, X. Zhou, *J. Chem. Educ.* **2016**, *93*, 345-350.

[21] J. Mei, N. L. C. Leung, R. T. K. Kwok, J. W. Y. Lam, B. Z. Tang, *Chem. Rev.* **2015**, *115*, 11718-11940.

[22] M. Gao, S. Li, Y. Lin, Y. Geng, X. Ling, L. Wang, A. Qin, B. Z. Tang, *ACS Sensors* **2016**, *1*, 179-184.

[23] a) A. D. Bochevarov, E. Harder, T. F. Hughes, J. R. Greenwood, D. A. Braden, D. M. Philipp, D. Rinaldo, M. D. Halls, J. Zhang, R. A. Friesner, *Int. J. Quantum Chem.* **2013**, *113*, 2110-2142; b) in *Jaguar*, Schrödinger, LLC, New York, NY, **2016**.

[24] a) C. A. Poynton, *Vol. 3299*, **1998**, pp. 232-249; b) J. van Rheenen, M. Langeslag, K. Jalink, *Biophys. J.* **2004**, *86*, 2517-2529; c) S. M. Sadeghi, A. Hatef, A. Nejat, Q. Campbell, M. Meunier, *J. Appl. Phys.* **2014**, *115*, 134315; d) C. Gui, E. Zhao, R. T. K. Kwok, A. C. S. Leung, J. W. Y. Lam, M. Jiang, H. Deng, Y. Cai, W. Zhang, H. Su, B. Z. Tang, *Chem. Sci.* **2017**, *8*, 1822-1830.

[25] a) C. Xie, Z. Zhang, B. Yang, G. Song, H. Gao, L. Wen, C. Ma, *Tetrahedron* **2015**, *71*, 1831-1837; b) T. Hirayama, S. Yamasaki, H. Ameku, T. Ishi-i, T. Thiemann, S. Mataka, *Dyes Pigm.* **2005**, *67*, 105-110.

10.1002/chem.201703253

WILEY-VCH

Layout 1:

FULL PAPER

Detecting biogenic amines: A new family of AIEgens provide a platform for simple, sensitive, bimodal detection of biogenic amine vapours produced by food fermentation. The colourimetric change allows for easy naked eye visualization, while fluorescence turn-on provides enhanced sensitivity for earlier indication, with a detection limit of 690 ppb for ammonia.

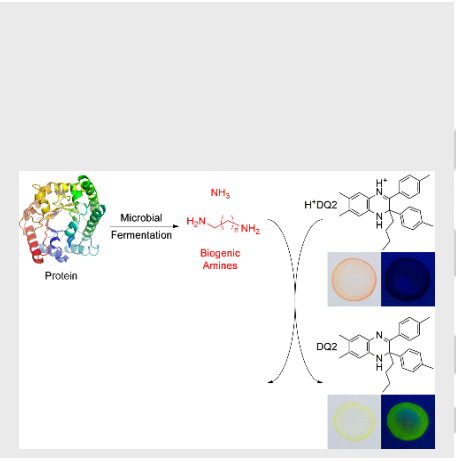

*Parvej Alam, Nelson L. C. Leung, Huifang Su, Zijie Qiu, Ryan T. K. Kwok, Jacky W. Y. Lam, and Ben Zhong Tang**

Page No. – Page No.

A Highly Sensitive Bimodal Detection of Amine Vapours Based on Aggregation Induced Emission of 1,2-Dihydroquinoxaline Derivatives